

A 3D CRACK EVOLUTION IN WELD METAL, BASE METAL AND THE TRANSITIONAL FUSION LINE UNDER A MIXED FATIGUE LOADING

Mahyar Asadi¹; Majid Tanbakuei Kashani¹; Mathew Smith¹
Chris Timbrell²; Ramesh Chandwani²; Arasch Rodbari²

Abstract: A limited number of automated algorithms and software are available that predict the 3D evolution of crack fronts in a mixed loading condition in welds in particular in the interface of weld and base metal i.e. fusion line. In this paper, the authors present a study of common low carbon steel pipe weld joints containing a crack detected in radiography films and embedded into a 3D FE pipe model that is constructed with different weld and base metal properties including different crack growth laws and fracture properties. Evolution of the detected crack front is predicted in 3D under mixed fatigue loading. This paper shows that a 3D model of crack growth captures the transient change of stress intensity factor along the crack front and therefore the immediate change in the direction of crack growth and the dynamic shape of crack can be predicted. A solution is also presented for handling the stress intensity factor on the boundary of weld metal and base metal when the crack front reaches the weld fusion line. From the structural integrity management viewpoint, the number of fatigue cycles, time for the crack to start growing, time to break to surface and leak-before-break, and the total time to final fracture are calculated. This paper shows that a fracture critical region such as welds with a high likelihood of service cracking or welding flaw can precisely be analyzed and life can be estimated to avoid early life failure in welded structures.

INTRODUCTION

Linear type defects are frequently detected in welds through radiography. They are mostly rejected by welding codes unless the Remaining Useful Life (RUL) is precisely calculated on a case-by-case basis in order to justify waive or repair decisions using the damage tolerance analysis codes such as API579, BS7910 and so on. Finite Element (FE) algorithms of life prediction are authorized by codes for the case-specific life calculation of structures containing defects. However, the existing capability of predicting crack behaviour in weld and welded structures, which are the most susceptible regions to contain a defect, are limited and not well automated to be practical.

A design philosophy development was started (1) based on fitness for service for welded structures subject to fatigue loading where we need to replace the idea of making a defect-free weld with the new understanding of weld processes that flaws will inevitably exist in

1 SKC Engineering (A division of Applus), 19165 94th Avenue, Surrey, BC, Canada, V4N 3S4
2 Zentech International Ltd., NW11 7RX, London, NW11 7RX, UK

welded structures. Conventional S/N diagrams can be useful for welds if and only if the severity of the defect is specified or can be assumed uniform from joint to joint. For example, porosity type defect in a butt weld subject to a uniform loading can be characterized by its volume, otherwise, the severity can change by size, shape, location and orientation of flaw in different joints and loading. An additional problem which may invalidate the use of S/N curves for welds is the microstructure and property notch effect from base metal to weld metal and lack of fracture data for weld metal materials which is also directional. In practice, critical crack size is much less than weld ligament and premature fracture can occur. Generally, S/N curves may not be used for planar defects and as a minimum an acceptable method should be capable of taking into account variation in local stress due to stress risers, flaw dimensions and shape parameters, and realistic sub critical crack size threshold. Therefore, a case-specific fracture mechanics analysis is required and representative material data needs to be fed into the analysis for calculating RUL for linear type defects.

Linear elastic fracture mechanics (LEFM) has been the primary approach to fatigue studies through using incremental crack extension per cycle and experimental data from ASTM E647. This leads to the damage tolerance life prediction that is based on crack's subcritical propagation life. Stress intensity factor (SIF or K) is the key parameter in characterizing a crack in LEFM. A widespread need for SIF solutions for typical geometry can be addressed by using Handbooks such as (2), (3), (4), (5) and standards for case applications such as BS7910, API579-1. The handbook solutions are typically extended through the superposition of SIFs for each type of loading. Although this is a common methodology for quick assessment of structural integrity, the main drawbacks are a) the labour-intensive process of incremental crack growth analysis, b) over-simplification of complex crack shape and loading conditions that are not directly addressed, c) user-subjective and non-deterministic analysis. Computer programs are being developed to mitigate these problems. A good approach for SIF solutions was developed based on weight function (6), (7) where the stress field is determined for an uncracked structure through a simple FEA analysis, and a weight function integrates over point load solution of cracked problem. A good understanding and practical application of this technique can be found by reviewing works done by Glinka, for example, in reference (8). For metal with elastic-plastic behaviour, a better approach was proposed (9) based on the energy release rate or J-Integral as the K equivalent for elastic plastic fracture mechanics. Similarly, Crack Tip Opening Displacement (CTOD) concept was introduced (10) as a comparable parameter to J-integral for elastic-plastic fracture mechanics for cases in which the plastic region at the tip of crack cannot be neglected. A good review of fracture characteristic parameters and interrelation are well summarized in (11). Increasing power of computers is now enabling a routine application of J-Integral and CTOD for complex loading and geometry at relatively short turnover time. However, the use of computational engineering of weld fracture and welded structures is among few fields where evolution of cracks has not yet well advanced. For example, a large variety of fracture resistant materials are available and employed to tolerate failure such as fatigue, creep, rupture and so on. Yet, failure has been observed to occur in our structures after a relatively low in-service life and is frequently reported in welds. These

demands lead to a need for more advanced algorithms that accommodate the local effect of welding and the crack behaviour in the weld region, base metal and at the fusion line. This paper presents an example of such a capability and explains how a weld region model needs to be prepared and analysed.

GEOMETRY, MATERIAL DATA AND LOADING CONDITION

The subject matter is a butt weld of structural steel pipe with OD = 57 mm and WT = 9.5 mm under a mixed loading of internal pressure of 0-758 bar at Low Frequency High Amplitude (LFHA) that occurs every hour and in between 644-758 bar at High Frequency Low Amplitude (HFLA) every minute (see Figure 1). The pipe, weld and initial crack geometry are shown in Figure 2 with a partial circumferential (0 -10 degree) Lack Of Fusion defect (LOF) from radiography examination. Ellipse major, minor axes lengths and inclination: 3.6mm, 1.8mm, 10° to pipe axis. Offset of ellipse centre from material interface at inner wall: axial 1mm, radial 1.5mm. Crack growth in the radial-axial plane was established by the methodology explained further in this paper. The maximum growth length was then calculated until the crack opened to the external surface (leak before break). At this point the SIF had become close to but still not reached the threshold of unstable growth (K_{1c}) and therefore additional crack growth could be tolerated in axial direction along the pipe axis under the hoop stress. Mechanical and Fracture properties used are given in Table 1 and Table 2. Note that the coefficients are for Paris law expressed in terms of K_{max} rather than ΔK .

Table 1 Mechanical Properties Used.

| | Tensile Modulus of Elasticity (GPa) | Tensile Yield Stress (MPa) | Poisson Ratio |
|------------|-------------------------------------|----------------------------|---------------|
| Weld Metal | 210 | 352 | 0.33 |
| Base Metal | 205 | 294 | 0.33 |

Table 2 Fracture Properties Used. Paris law C and m are for da/dn m/cycle, K MPa-m^{1/2}.

| | R = 0 | | | | R = 0.85 | | | |
|------------|------------------------|-----|----------|----------|------------------------|-----|----------|----------|
| | C | m | K_{th} | K_{1c} | C | m | K_{th} | K_{1c} |
| Weld Metal | 1.35×10^{-12} | 3.6 | 6 | 65 | 1.13×10^{-16} | 5.8 | 21 | 65 |
| Base Metal | 1.60×10^{-14} | 4.8 | 5.5 | 65 | 1.34×10^{-18} | 7.0 | 21 | 65 |

MODELLING PRINCIPLE

The fatigue crack growth prediction presented here is based on linear elastic fracture mechanics and finite element techniques implemented within the Zencrack software (12). This code uses a sequence of underlying 3D finite element analyses, in this case via Abaqus/Standard (13), to calculate and refresh the relevant fracture mechanics parameters as the crack shape evolves. The techniques are general with all crack growth material properties and the fatigue load history defined as part of the Zencrack input data. Crack growth integration and remeshing as the crack advances are controlled by Zencrack. For the weld in question the approach provides a means of assessing behaviour for a crack which crosses a weld fusion line.

The starter crack for the analysis is a fully embedded ellipse within the weld material being oriented as shown in Figure 2. It transitions to a breakthrough crack which is modelled in a second analysis (see Figure 3). For both phases the finite element model consists of a pipe length of 123.5mm (2.6x the mean wall diameter) containing a combination of fully integrated brick and tet elements (Abaqus types C3D20 and C3D10). 180 degrees of the pipe is modelled with the crack lying on the symmetry plane. Internal pressure and end cap pressure are applied. For the breakthrough crack the internal pressure load is also applied on the crack face. The initial crack for each of the elliptic and breakthrough phases is inserted by Zencrack into the user-supplied uncracked models by replacement of a line of “crack-blocks”. These crack-blocks introduce the detail of the crack front and include the rings of elements required around the crack front to perform contour integral evaluation. The collapsed brick elements at the crack front contain a single node at each crack front location with the radial midside nodes moved to the quarter point position i.e. standard practice for LEFM modelling. The elliptic and breakthrough models contain 96 and 51 elements respectively along their crack fronts.

The mesh density has been assessed via studies on an uncracked specimen and a more refined version of the cracked models containing twice as many elements along the crack front.

The more interesting aspect of the modelling relates to the material interfaces at the weld fusion line. Generally in a numerical model of this type there are two competing and incompatible sets of requirements regarding the element definitions; 1) the element shape requirements to define the crack front and 2) the element boundary requirements to define the material interfaces. An attempt to satisfy both requirements leads to significant compromises in the mesh to the extent that certain configurations cannot reasonably be modelled. To resolve these competing requirements the crack modelling takes precedence with element boundaries, by necessity, being allowed to traverse the fixed locations of the material interfaces. The material properties are then applied via user subroutines:

- 1) For the Abaqus analyses the user defined field subroutine, usfld, is used to assign material properties on a per integration point basis according to the physical position of each integration point. A typical cracked mesh with the material field variable

contours 1 and 2 is shown in Figure 3. The approximate nature interface lines of this plot is a consequence of the element distribution and extrapolation and averaging of integration point values to the nodes to produce the contour plot – all integration point values for the material id are exactly 1 or 2.

- 2) For the crack growth integration process in Zencrack the subroutine `user_material_id` assigns a material id to each corner node on the crack front at the start of an integration step using the current physical position of each node.

The method of calculation of fracture mechanics parameters for nodes near the material interface avoids theoretical complexities of the discontinuity in the stress field at the interface by taking a pragmatic view:

- 1) The calculation of contour integrals (via the Abaqus `*CONTOUR INTEGRAL` option) and stress intensity factors by conversion of nodal displacements follow the normal procedures that would be used in a single material model with the appropriate data for one or both materials being used as required. It is accepted that there will be some approximation when a crack front node is very close to the interface.
- 2) Studies for inclined cracks in multi-material plates have shown that the effect of the interface is highly localised in terms of global behaviour of the crack shape. The approximation in the modelling of this local effect does not have a globally significant effect on the overall crack behaviour.
- 3) Small approximations in the numerical approach must be weighed against the reality that fusion lines are not perfectly straight boundaries with instantaneous change of material properties.

When the elliptic crack shape extends close to the inner wall there comes a point when re-meshing is no longer possible due to the proximity of the crack to the inner surface. At this point the crack shape is manually transitioned to a breakthrough crack by maintaining the majority of the crack position and breaking the crack through to have two distinct ends at the inner wall. This assumed initial breakthrough shape quickly returns to the “natural” crack shape as the breakthrough phase starts up.

CRACK GROWTH LIFE CALCULATION METHODOLOGY

The crack growth methodology uses a series of finite element analyses with each modelling progressively larger crack sizes. The integration scheme uses energy release rate values, G , rather than stress intensity factors with appropriate conversion to use the supplied growth laws. After each finite element analysis of a crack position a new distribution of energy release rates is available at each corner node position on the crack front. A “forward predictor” scheme is used to take account of changes in G over the previous integration step when calculating growth for the current step. This scheme also controls the maximum allowable da increment between finite element steps to prevent instability developing in the

crack shape. The integration of crack position through the load history is carried out for each corner node on the crack front in a two-stage process such that all nodes are advanced by the same increment of load spectrum passes but with the likelihood of different increments in da . This allows the correct crack shape to develop taking full account of any threshold effect that may be relevant to only parts of the crack front.

A single pass of the applied load spectrum consists of 1 cycle of LFHA load followed by 60 cycles of HFLA load. The total growth rate over a single load spectrum is calculated by considering each of these load blocks separately. This allows the separate growth laws and threshold conditions for the two load blocks to be treated independently and consistently as the crack advancement is being calculated – a load block may contribute no growth if it is below threshold or have a da/dn value determined by the current K_{max} and appropriate growth law if it is above threshold. For example, in the early stages of the analysis the LFHA cycle may be above threshold but the HFLA cycles are below threshold and do not contribute to the growth. Later on, each part of the loading may contribute to the growth but this combined effect will start to occur at different total spectrum counts on different parts of the crack front. As the crack size is increased during the integration process the forward predictor scheme adjusts the current value of K_{max} based on growth accrued since the previous finite element analysis i.e. there is an assumption of linear variation of G between finite element analyses rather than a constant value of G .

RESULTS AND DISCUSSION

Figure 4 to Figure 7 show a selection of profiles from the elliptic and breakthrough phases of growth. The K values in the elliptic phase do not exceed the threshold value $K_{th}=21 \text{ MPam}^{1/2}$ at which the HFLA load cycle becomes activated. Therefore, analyses of the elliptic phase with the LFHA and HFLA loading included in the spectrum definition produce the same results as an analysis with only LFHA loading. For this reason only one set of elliptic phase results are presented. During the elliptic phase the crack front crosses one fusion line interface beyond which the growth rate is reduced.

The breakthrough analyses with the two loading scenarios begin with slightly different growth near the inner wall due to exceedance of the $K_{th}=21 \text{ MPam}^{1/2}$ threshold close to the inner wall which introduces an effect of the HFLA into that analysis. However, this is a local effect near the surface (see Figure 8) and as the crack develops the maximum K value drops back below the HFLA threshold. There is then a region of growth with all crack front nodes below threshold and similarity in the profiles for the two analyses until the overall crack size is sufficient that the threshold is again exceeded. From this point the analysis with HFLA loading included shows higher growth due to the contributions from the HFLA cycles. The effect is more pronounced in the weld due to the higher growth rate associated with the weld properties when K is in the region 21 to 40 $\text{MPam}^{1/2}$.

The following points are noted with regard to the various results plots:

- The initial ellipse has small regions of zero growth at the extremities of the major axis (see Figure 6 and Figure 7). This occurs when K is below the $K_{th}=6 \text{ MPam}^{1/2}$ threshold for LFHA loading. As the crack grows the threshold becomes exceeded at all points and the entire crack front advances.
- Figure 6 and Figure 7 show the location of the maximum K for each crack profile calculated during the analyses. Note that for clarity only a selection of the profiles are drawn as lines. Also, the two breakthrough phases complete in different numbers of finite element runs due to smaller steps being required to maintain stability of the crack shape once the HFLA loading is activated. Hence a higher number of points are shown in Figure 6 and Figure 7.
- Local changes occur in the crack shape near the fusion line and at the boundary of regions in which HFLA cycles is activated for some nodes but not for adjacent nodes. These types of changes in shape can clearly be seen in Figure 5.
- Localised crack shape changes as the HFLA effect starts cause small local variations in the K values which manifest themselves as small oscillations in the maximum K values (blue line on Figure 9 at around 225,000 spectrum passes). There can also be a small local effect as the crack crosses the fusion line at the inner wall (red line on Figure 9 at around 250,000 spectrum passes).
- Figure 8 and Figure 9 show an apparent general increase in K of around $5.5 \text{ MPam}^{1/2}$ once breakthrough occurs. This is due to the introduction of crack face pressure once the crack opens to the inner surface.

CONCLUSION

Today's fracture analysis requires a case-specific problem-solving capability and needs to precisely compute crack evolution using dynamic evolution of crack fronts in order to justify making structural integrity decisions particularly for welded structures. This paper presents an approach that predicts the dynamic evolution of crack shape over the interface of weld and base metal i.e. fusion line under mixed loading condition. We also proposed to use overall K_{max} of crack front nodes to monitor and detect the critical integrity moments such as coalescence, crack opening to surfaces, and leak before break. For example a plot of K_{max} vs. the number of load spectrum cycles can properly characterize the critical moments in cracking life.

REFERENCE LIST

- (1) Maddox, S J. Assessing the Significance of Flaws in Welds Subject to Fatigue. Welding Research Supplement. Houston TX : AWS, 1974, pp. 401-s - 404-s.

Engineering Structural Integrity Assessment - ESIA14, in conjunction with
the 2017 International Symposium on Structural Integrity – ISSI2017

- (2) Tada, Hiroshi, Paris, Paul C and Irwin, George R. The Stress Analysis of Cracks Handbook, 3rd ed. s.l. : ASM, 1973.
- (3) Sih, George C. Handbook of Stress-Intensity Factors: Stress-intensity Factor Solutions and Formula for Reference. s.l. : Lehigh University, 1973.
- (4) Rooke, David P. Compendium of stress intensity factors. s.l. : H.M.S.O , 1976.
- (5) Murakami, Yukitaka. Stress intensity factors handbook. s.l. : Elsevier Science Limited, 1987.
- (6) A Novel Principle for the Computation of Stress Intensity Factor. Bueckner, H F. 1970, Math. Mech, Vol. 50, pp. 529-546.
- (7) Some Remarks on Elastic Crack-tip Stress Field. Rice, J R. 1972, Int'l J. Solid Struct., Vol. 8, pp. 751-758.
- (8) Calculation of Stress Intensity Factors and Crack Opening Displacements for Cracks Subjected to Complex Stress Fields. Kiciak, A, Glinka, G and Burns, D J. 2003, Transaction of the ASME, Vol. 125, pp. 260-266.
- (9) A Path Independent Integral and the Approximate Analysis of Strain Concentration by Notches and Cracks. Rice, J R. 1968, J. Appl Mech, Vol. 35, pp. 379-386.
- (10) Application of Fracture Mechanics at and Beyond General Yielding. Well, A A. 1963, Br. Weld, Vol. 10, pp. 563-570.
- (11) Zhu, xian-Kui and Joyce, James A. Review of Fracture Toughness (G, K, J, CTOD, CTOA) Testing and Standardization. s.l. : US Navy Research, 2012.
- (12) Zencrack 8.1, . London, U.K.. : Zentech International Limited, 2017.
- (13) Abaqus 2017,. Providence, Rhode Island, U.S.A. : Dassault Systèmes Simulia Corp. (SIMULIA), 2016.

FIGURES

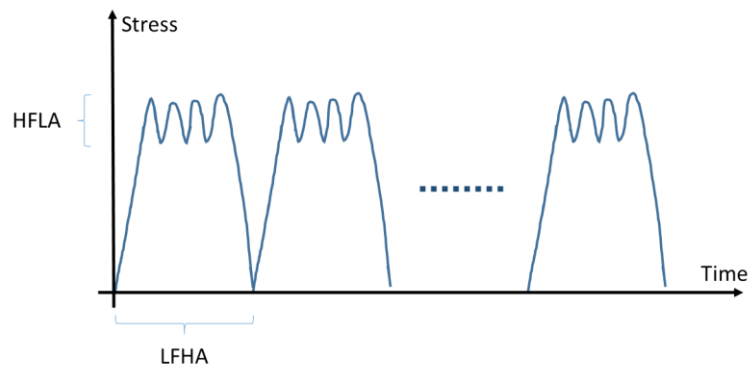


Figure 1 LFHA (Low Frequency High Amplitude Cycle) at $R=0$, and HFLA (High Frequency Low Amplitude Cycle) at $R= 0.85$.

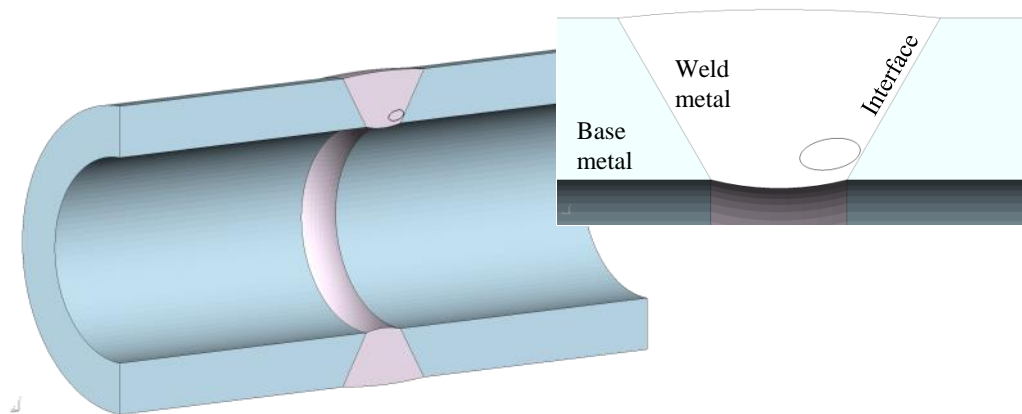


Figure 2 Definition of the geometry and the initial crack.

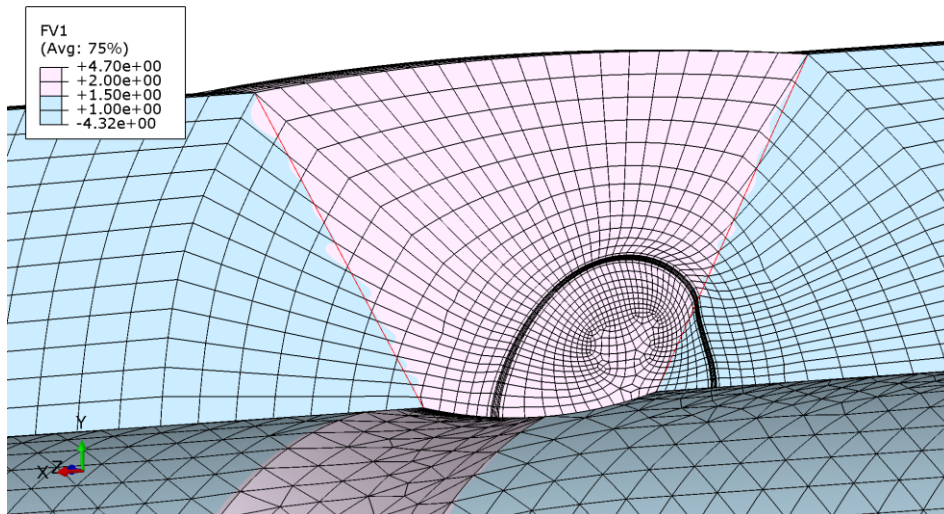


Figure 3 Typical mesh at the crack region showing material id (1 or 2) field variable.

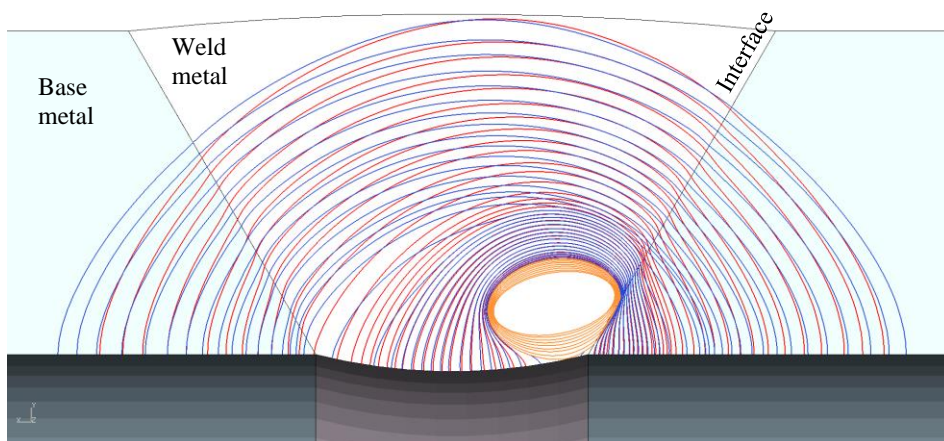


Figure 4 Growth profiles – LFHA only (orange & red) and LFHA & HFLA (orange & blue).

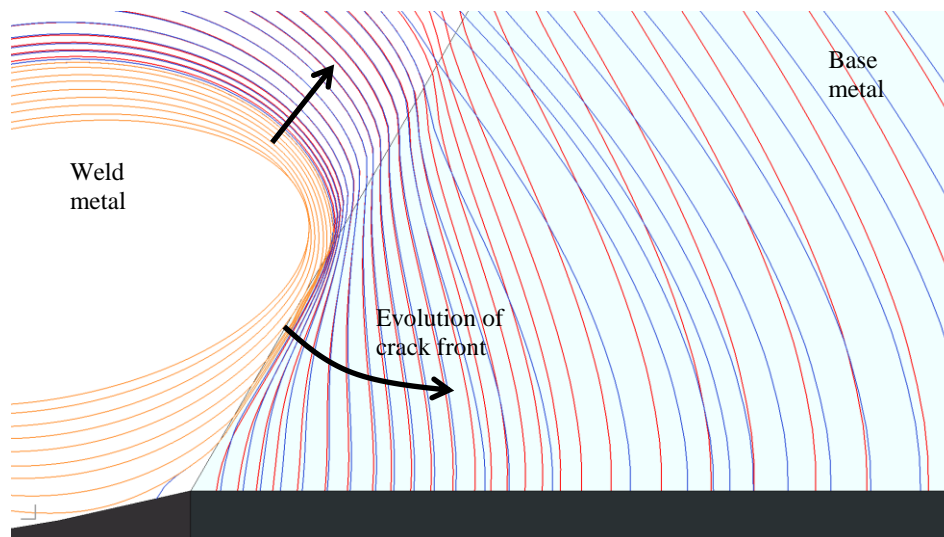


Figure 5 Growth profiles near the fusion line– LFHA only (orange & red) and LFHA & HFLA (orange & blue).

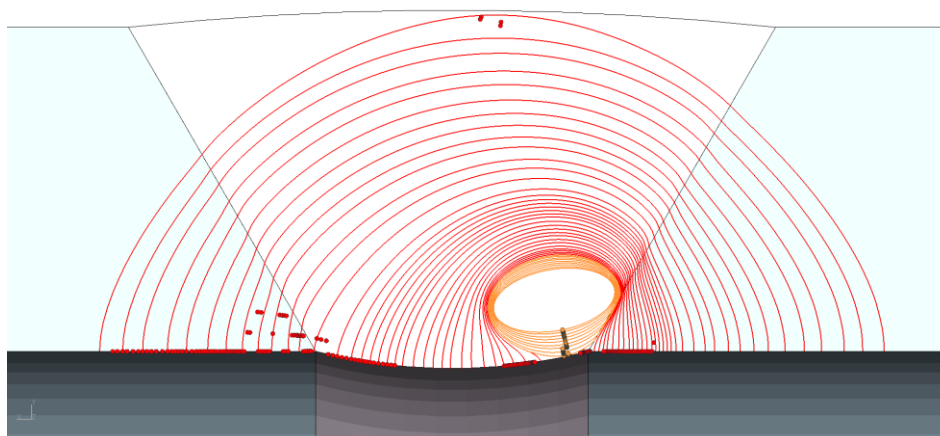


Figure 6 Growth profiles with markers for K_{max} positions – LFHA only.

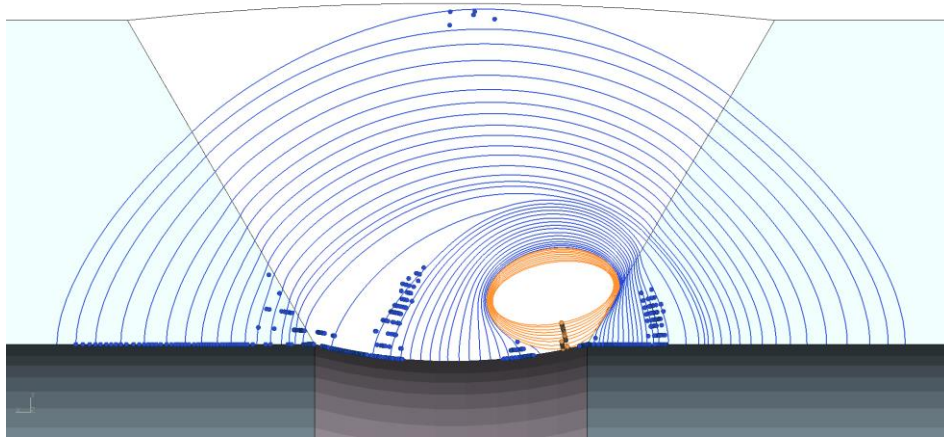


Figure 7 Growth profiles with markers for K_{max} positions – LFHA & HFLA.

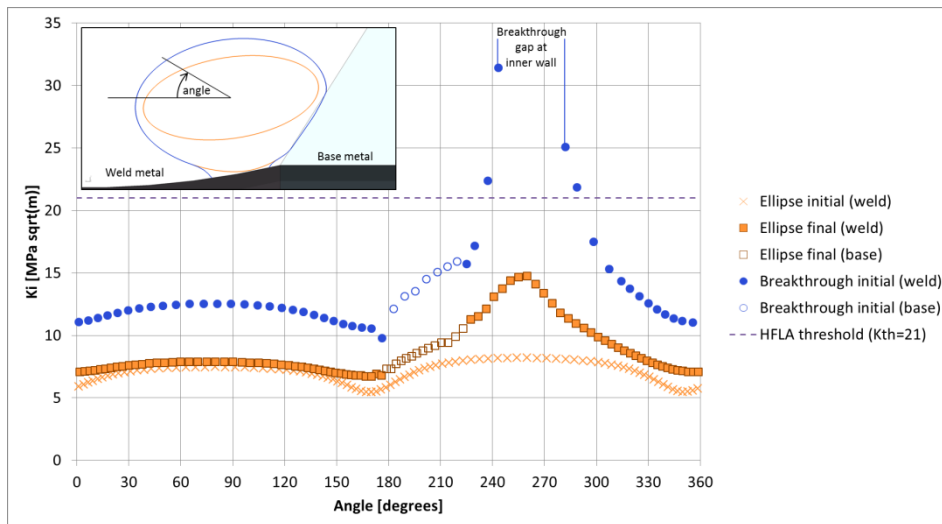


Figure 8 K_i distributions along the crack front for ellipse phase and initial breakthrough crack.

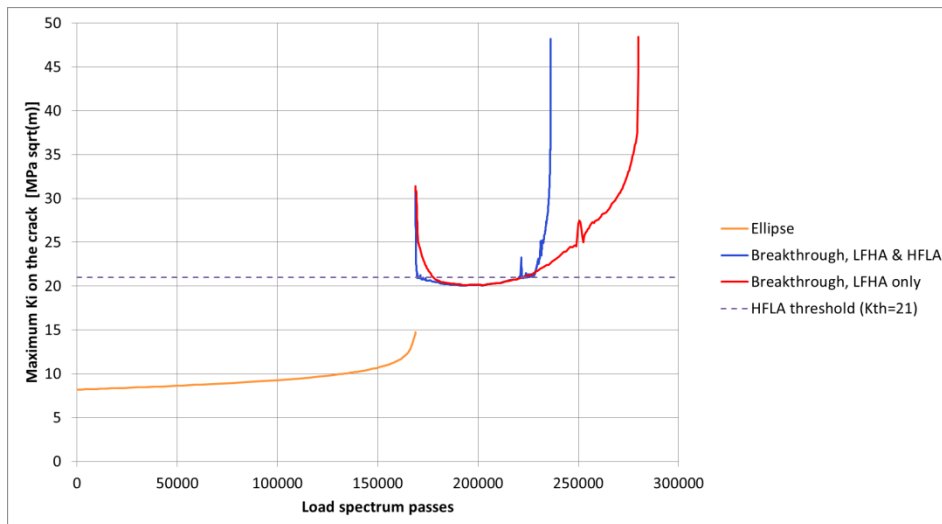


Figure 9 Maximum K_i on the crack front vs load spectrum passes.